OPEN

Molecular Psychiatry (2015) 20, 1179–1187

www.nature.com/mp

ORIGINAL ARTICLE

Amyloid-PET predicts inhibition of *de novo* plaque formation upon chronic γ-secretase modulator treatment

M Brendel[1,10], A Jaworska[2,3,10], J Herms[2,4,10], J Trambauer[5,10], C Rötzer[1], F-J Gildehaus[1], J Carlsen[1], P Cumming[6], J Bylund[7], T Luebbers[8], P Bartenstein[1,4], H Steiner[2,5,10], C Haass[2,4,5,10], K Baumann[9,10] and A Rominger[1,4,10]

In a positron-emission tomography (PET) study with the β-amyloid (Aβ) tracer [^{18}F]-florbetaben, we previously showed that Aβ deposition in transgenic mice expressing Swedish mutant APP (APP-Swe) mice can be tracked *in vivo*. γ-Secretase modulators (GSMs) are promising therapeutic agents by reducing generation of the aggregation prone $Aβ_{42}$ species without blocking general γ-secretase activity. We now aimed to investigate the effects of a novel GSM [8-(4-Fluoro-phenyl)-[1,2,4]triazolo[1,5–a]pyridin-2-yl]-[1-(3-methyl-[1,2,4]thiadiazol-5-yl)-piperidin-4-yl]-amine (RO5506284) displaying high potency *in vitro* and *in vivo* on amyloid plaque burden and used longitudinal Aβ-microPET to trace individual animals. Female transgenic (TG) APP-Swe mice aged 12 months (m) were assigned to vehicle (TG-VEH, $n=12$) and treatment groups (TG-GSM, $n=12$), which received daily RO5506284 (30 mg kg^{-1}) treatment for 6 months. A total of 131 Aβ-PET recordings were acquired at baseline (12 months), follow-up 1 (16 months) and follow-up 2 (18 months, termination scan), whereupon histological and biochemical analyses of Aβ were performed. We analyzed the PET data as VOI-based cortical standard-uptake-value ratios (SUVR), using cerebellum as reference region. Individual plaque load assessed by PET remained nearly constant in the TG-GSM group during 6 months of RO5506284 treatment, whereas it increased progressively in the TG-VEH group. Baseline SUVR in TG-GSM mice correlated with Δ%-SUVR, indicating individual response prediction. Insoluble $Aβ_{42}$ was reduced by 56% in the TG-GSM versus the TG-VEH group relative to the individual baseline plaque load estimates. Furthermore, plaque size histograms showed differing distribution between groups of TG mice, with fewer small plaques in TG-GSM animals. Taken together, in the first Aβ-PET study monitoring prolonged treatment with a potent GSM in an AD mouse model, we found clear attenuation of *de novo* amyloidogenesis. Moreover, longitudinal PET allows non-invasive assessment of individual plaque-load kinetics, thereby accommodating inter-animal variations.

Molecular Psychiatry (2015) **20,** 1179–1187; doi:10.1038/mp.2015.74; published online 9 June 2015

INTRODUCTION

With its exponentially increasing incidence as a function of age, Alzheimer's disease (AD) has become the most common form of dementia, and is imposing a significant burden on health care systems of societies with aging populations.[1] Neurofibrillary tangles and amyloid plaques are the histologically characterizing hallmarks of AD.[2] The principal component of amyloid plaques, the β-amyloid (Aβ) peptide, is a heterogeneous cleavage product of the Aβ precursor protein (APP) generated by β- and γ-secretase. Of the several Aβ variants the $Aβ_{42}$ species is widely believed to be a key factor of the disease.[3] Current therapeutic options for AD include acetylcholinesterase inhibitors[4] and NMDA receptor antagonists,[5] both of which provide some transient amelioration of cognitive symptoms, but without any disease-modifying effects.[6,7] Consequently, there is an urgent need for disease-modifying treatments such as those targeting amyloidosis. γ-Secretase inhibitors (GSIs) suppress intestinal cell differentiation and also lymphopoiesis, owing to inhibition of Notch signaling[8] and a large phase III clinical trial was terminated owing to severe side effects.[9] However, γ-secretase inhibition may still be a hopeful approach,[10] although pharmaceutical companies may stay away from such efforts. First generation unselective GSIs affect dendritic spine plasticity,[11] which may explain reports of cognitive deterioration in AD patients with long-term GSI treatment.[9,12] Interestingly, however, Notch-sparing GSIs do not seem to affect spines.[13] In contrast to GSIs, γ-secretase modulators (GSMs) shift Aβ production from the more toxic $Aβ_{42}$ to shorter forms, which are less apt to form amyloid aggregates. This favorable modulation of γ-secretase is obtained without affecting signaling cleavages of Notch or other critical substrates.[14–16] In recent years highly potent GSMs have been developed, which target γ-secretase in the N-terminal fragment of its catalytic subunit presenilin.[17–20] Owing to their profile of modulating rather than inhibiting γ-secretase cleavage, GSMs hold great potential as therapeutics with improved safety, reducing the underlying disease pathology which might ultimately alter the course of the disease.

Recent testing of several GSMs in transgenic mice showed reduced plaque area fraction in cortex and hippocampus, as well

[1]Department of Nuclear Medicine, Ludwig-Maximilians-University of Munich, Munich, Germany; [2]DZNE—German Center for Neurodegenerative Diseases, Munich, Germany; [3]Laboratory of Neurodegeneration, International Institute of Molecular and Cell Biology, Warsaw, Poland; [4]Munich Cluster for Systems Neurology (SyNergy), Munich, Germany; [5]Biomedical Center (BMC), Ludwig-Maximilians-University of Munich, Munich, Germany; [6]Department of Psychiatry, University of Oslo, Oslo, Norway; [7]Roche Pharma Research and Early Development, Pharmaceutical Sciences, Roche Innovation Center Basel, F. Hoffmann-La Roche Ltd., Basel, Switzerland; [8]Roche Pharma Research and Early Development, Small Molecule Research, Roche Innovation Center Basel, F. Hoffmann-La Roche Ltd., Basel, Switzerland and [9]Roche Pharma Research and Early Development, Neuroscience Discovery, Roche Innovation Center Basel, F. Hoffmann-La Roche Ltd., Basel, Switzerland. Correspondence: Professor A Rominger, Department of Nuclear Medicine, Ludwig-Maximilians-University of Munich, Marchioninistr. 15, Munich 81377, Germany.
E-mail: axel.rominger@med.uni-muenchen.de
[10]These authors contributed equally to this work.
Received 22 December 2014; revised 31 March 2015; accepted 13 April 2015; published online 9 June 2015

as lower plaque density during chronic treatment.[21–23] A number of chronic GSM treatment studies in Tg2576 mice revealed a dose-dependent reduction of brain $A\beta_{42}$ levels,[21,22,24,25] whereas Rogers *et al*.[24,25] also observed a significant decrease of total Aβ levels.

As shown in previous studies, small animal positron-emission tomography (PET) is a suitable non-invasive tool for monitoring the amyloid plaque load of transgenic mice *in vivo*,[26–28] yielding excellent correlations with histological or biochemical assessments. As these transgenic models entail a large inter-animal heterogeneity with regard to extent of the pathology,[29] conducting longitudinal PET studies in individual animals is highly desirable.[27] In accordance with animal protection regulations such studies may also help to reduce the number of animals required.

Given this background, we aimed to monitor the progression of amyloidosis *in vivo* in APP-Swe mice treated for 6 months with the novel GSM [8-(4-Fluoro-phenyl)-[1,2,4]triazolo[1,5–a]pyridin-2-yl]-[1-(3-methyl-[1,2,4]thiadiazol-5-yl)-piperidin-4-yl]-amine (RO5506284) by means of small animal amyloid PET with [^{18}F]-florbetaben followed by *ex vivo* multimodal histological and biochemical assessment. We found that the GSM treatment effectively lowered *de novo* amyloidogenesis over time and that longitudinal amyloid-PET monitoring effectively copes with the known inter-animal variability making it superior to classical end point analyses.

MATERIALS AND METHODS

Synthesis of RO5506284

RO5506284 (Figure 1a) was prepared as described in the patent literature.[30]

GSM potency and selectivity

In vitro drug potency determination was performed in H4 and N2A cells overexpressing APP containing the Swedish mutation (K670N, M671L). Dose-response curves to determine IC_{50} values for Aβ modulation by RO5506284 were generated as outlined previously[31] with the following modification: Quantification of human or mouse $A\beta_{42}$ levels in cell culture supernatant were performed using AlphaLISA kit (PerkinElmer, Waltham, MA, USA) according to the manufacturer's instructions. The cellular Notch reporter assay used a stably transfected HEK293 cell line expressing human Notch1 and a luciferase reporter[32] (further details are listed in Supplementary Information).

Animals

All experiments were performed in compliance with the Swiss federal regulations (acute treatment arm) and National Guidelines for Animal Protection, Germany, (chronic treatment arm) with approval of the local animal care committee of the Government of Oberbayern (Regierung Oberbayern), and overseen by a veterinarian. Transgenic APP-Swe mice overexpress human APP with the Swedish mutation driven by the mouse Thy1.2 promoter[33] (further details are listed in Supplementary Information). Age-matched C57Bl/6 mice served as controls.

Acute treatments and dose finding

For acute *in vivo* treatment of APP-Swe mice, the compound was administered once per os (gavage) at different doses from 3–100 mg kg^{-1} and different time points from 2–24 h. Vehicle for the acute treatment was 5% ethanol (VWR Prolabo, Darmstadt, Germany), and 10% solutol (BASF Chemtrade GmbH, Burgbernheim, Germany) dissolved in sterile water (Baxter, Compton, UK). For chronic treatment, animals were administered a daily dose of 30 mg kg^{-1} per os (gavage) over a period of 6 months. Vehicle for chronic treatment was 0.9% (w/v) NaCl in 0.3% (v/v) Tween-80 microsuspended in sterile water, thus avoiding potential effects of long-term ethanol administration. Mice were killed by cervical dislocation at the indicated time after a single oral administration of drug or vehicle. Brains were collected, frozen on dry ice and stored at −80 °C until analysis of soluble cerebral Aβ. For the determination of soluble Aβ levels, a previously described procedure was used[34] (details are listed in Supplementary Information). Correlation of *in vivo with in vitro* potency was estimated using pharmacokinetic (PK) and pharmacodynamics (PD) analysis, plasma protein binding determination and P-glycoprotein assessment (details are listed in Supplementary Information).

Chronic treatment arm

Groups of 24 female APP-Swe transgenic (TG) and C57Bl/6 wild-type (WT) mice were randomized to either treatment (TG-GSM; WT-GSM) or vehicle (TG-VEH; WT-VEH) groups at the age of 12 months (Figure 2a), based on assumptions for a type I error $\alpha = 0.05$, a power of 0.8 and a drop-out rate of 15% during follow-up. At 12 months, a baseline [^{18}F]-florbetaben-PET scan (Aβ-PET) was performed, followed by initiation of daily oral RO5506284 treatment or vehicle, for a period of 6 months. Follow-up Aβ-PET-scans were acquired at 16 and 18 months of age, the termination of the study. Mice were killed after completion of the final Aβ-PET-scan, and brains were histologically and biochemically analyzed. Table 1 provides a detailed overview on study groups and analyses performed.

GSM plasma level assessment

Described in Supplementary Information.

Aβ extraction from brain and quantification

Upon completion of the final Aβ-PET recording, mice were killed while deeply anesthetized. The brains were removed and bisected. Hemispheres intended for biochemical analysis were directly frozen by immersion in liquid nitrogen. The soluble Aβ pool was extracted as described above and in Supplementary Information. For detailed description on extracting the insoluble Aβ pool and determination of Aβ species see Supplementary Information.

Aβ-PET

Aβ-PET image acquisition, reconstruction and analysis followed a standardized protocol, as previously published[27] and is described in more detail in the Supplementary Information. Corresponding $SUVR_{CTX/CBL}$ values were calculated for all groups at each Aβ-PET-scan and individual longitudinal changes were calculated between baseline and follow-ups at 16 and 18 months of age (Δ%-$SUVR_{CTX/CBL}$).

Histochemical analyses

Fibrillary Aβ plaques were stained with the fluorescent dye methoxy-X04 (0.01 mg ml^{-1} in phosphate-buffered saline at pH 7.4 for 15 min).[35] Further details are described in Supplementary Information. Plaque load was calculated as the summed area of all plaques relative to the frontal cortex area. Plaque density was calculated as the number of plaques relative to frontal cortex area.[27] These analyses were performed by an operator blind to the Aβ-PET results.

Statistics

Group comparisons of VOI-based Aβ-PET results were performed with multivariate analysis of variance using IBM SPSS Statistics (Version 22.0, Chicago, IL, USA). Histology and biochemistry data were compared between treated and untreated transgenic mice by multivariate analysis of covariance using Aβ-PET baseline estimates as a covariate. For correlation analyses, Pearson coefficients of correlation (r) were calculated. Plaque size distributions were compared with a χ^2 test followed by the Kolmogorov–Smirnov test with Prism V5.04 software (GraphPad Software, San Diego, CA, USA). A Shapiro–Wilk test was performed to verify normal distribution of sample values. A threshold of $P < 0.05$ was considered to be significant for rejection of the null hypothesis.

RESULTS

RO5506284 is a potent GSM

We first characterized the properties of RO5506284 (Figure 1a), a potent GSM, which selectively lowers $A\beta_{42}$ and $A\beta_{40}$ whereas increasing the $A\beta_{38}$ concentrations. This profile is typical for many GSMs of this compound class, which is characterized by a bridged-aromatic scaffold.[17,22,31,36] The IC_{50} for inhibition of $A\beta_{42}$ production in human H4 neuroglioma cells and mouse N2A cells both overexpressing human APP-Swe were 25.7 nM (±7.0 s.e.m., $n = 4$)

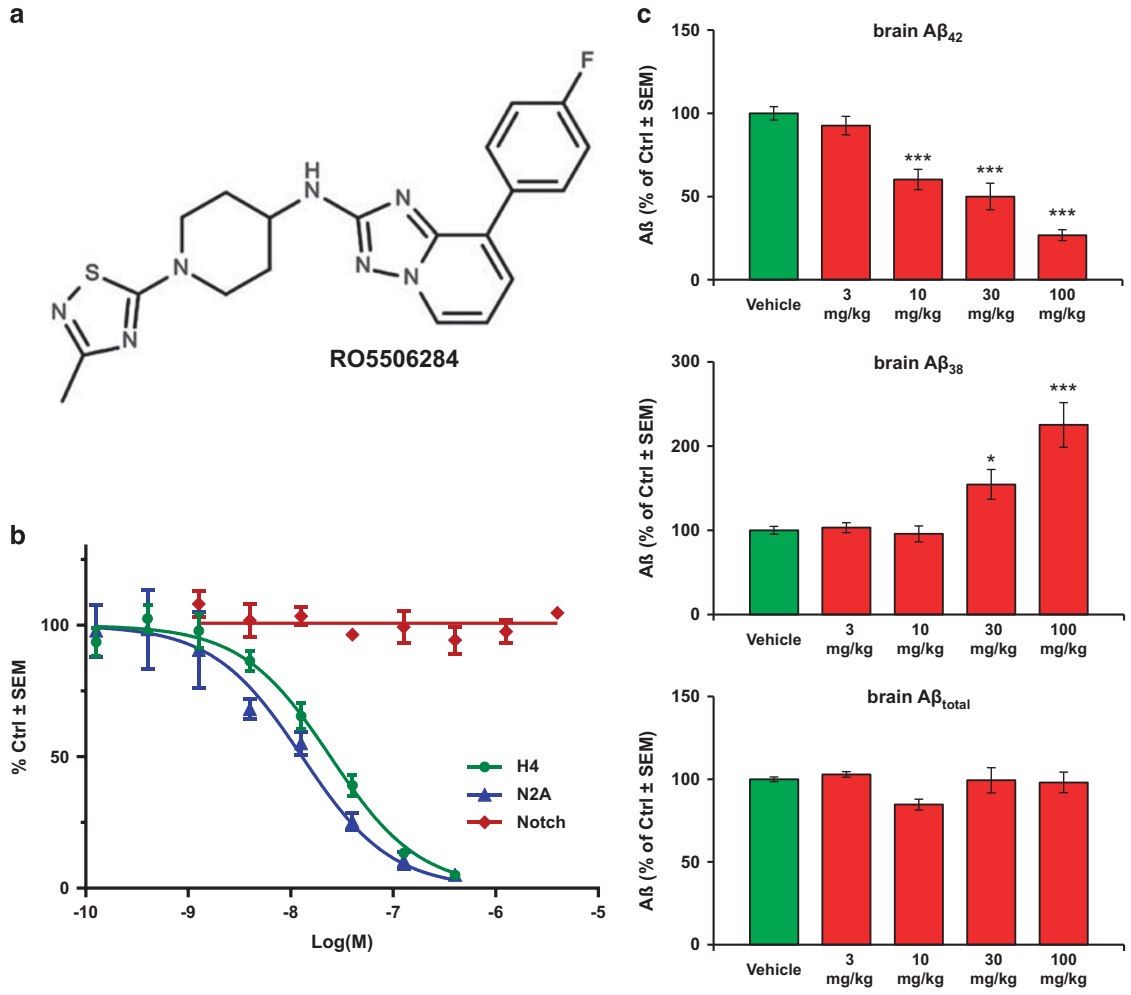

Figure 1. (**a**) Chemical structure of RO5506284 ([8-(4-Fluoro-phenyl)-[1,2,4]triazolo[1,5–a]pyridin-2-yl]-[1-(3-methyl-[1,2,4]thiadiazol-5-yl)-piperidin-4-yl]-amine). (**b**) *In vitro* potency of RO5506284 in human H4 and mouse N2A cells overexpressing Swedish mutant APP on $A\beta_{42}$ secretion; and effect on Notch processing in the HEK293 cell reporter assay. (**c**) Reduction of brain $A\beta_{42}$ was determined in an acute study where the animals were killed 4 h post-treatment. Each bar represents the mean of $n = 5$ ($n = 4$ at 100 mg kg^{-1}) animals. Young 3-month old, pre-amyloid Tg mice were used for this study to determine the changes of soluble brain Aβ following acute γ-secretase modulation with RO5506284. A dose-dependent decrease of brain $A\beta_{42}$ (upper panel) and a corresponding increase of $A\beta_{38}$ (mid panel) can be observed, without major effect in total Aβ levels (lower panel). *indicates statistically significant at $P < 0.05$; ***indicates statistically significant at $P < 0.001$.

and 13 nM (±3.1 s.e.m., $n = 2$), respectively. No inhibition of Notch processing was observed up to concentrations of 4 μM ($n = 4$; Figure 1b).

Acute *in vivo* effects and dose finding

In acute *in vivo* treatment studies, RO5506284 showed a dose-dependent decrease of brain $A\beta_{42}$ production in young APP-Swe mice after a single oral dose. $A\beta_{42}$ levels were significantly reduced by 40, 48 and 73% at 4 h after treatment with single doses of 10, 30 and 100 mg kg^{-1} per os ($P < 0.001$, tested by one-way analysis of variance, Dunnett's multiple comparisons test), respectively. Corresponding increases of brain $A\beta_{38}$ levels were observed, whereas no major change of total brain Aβ levels were observed (Figure 1c).

The *in vivo* total plasma IC_{50} was estimated to be 1340 ng ml^{-1} and the free plasma IC_{50} was calculated to be 15 nM which is in good correlation of *in vitro* potency of 13 nM. On the basis of the PK/PD analysis, a single dose of 30 mg kg^{-1} was anticipated to produce a maximal $A\beta_{42}$ reduction of ~60% at 3 h post dose, a reduction of 50% at 4 h and a return to baseline after 24 h.

Chronic GSM treatment effects

The study plan of the chronic treatment arm is outlined in Figure 2a. Details of animal drop outs are provided in Supplementary Information. PK/PD analysis based on RO5506284 exposure in APP-Swe mice after the last day of dosing (similar PK in WT was observed) and generated acute brain $A\beta_{42}$ effect data suggested an average reduction of brain $A\beta_{42}$ levels over the treatment period in the range of 20–25% (Figure 2b). Upon daily chronic treatment with 30 mg kg^{-1} RO5506284 for 6 months, the concentration of insoluble $A\beta_{42}$ was 40% lower in the TG-GSM vs the TG-VEH group ($P < 0.05$; Figure 2c), whereas amounts of the other Aβ species did not differ significantly (Table 1). Our randomization of TG mice resulted in allocation of three animals to the TG-GSM group with elevated Aβ-PET (> 2 s.d.) at the start of treatment (labeled with arrows in Figure 2c). This required scaling of results to the individual baseline amyloid level determined by PET (see below) using multivariate analysis of covariance, thereby accounting for much of the inter-animal variability. Upon making this adjustment, $A\beta_{42}$ was considerably lower in TG-GSM than in TG-VEH (−56%; $P < 0.001$; Figure 2d), whereas amounts of the

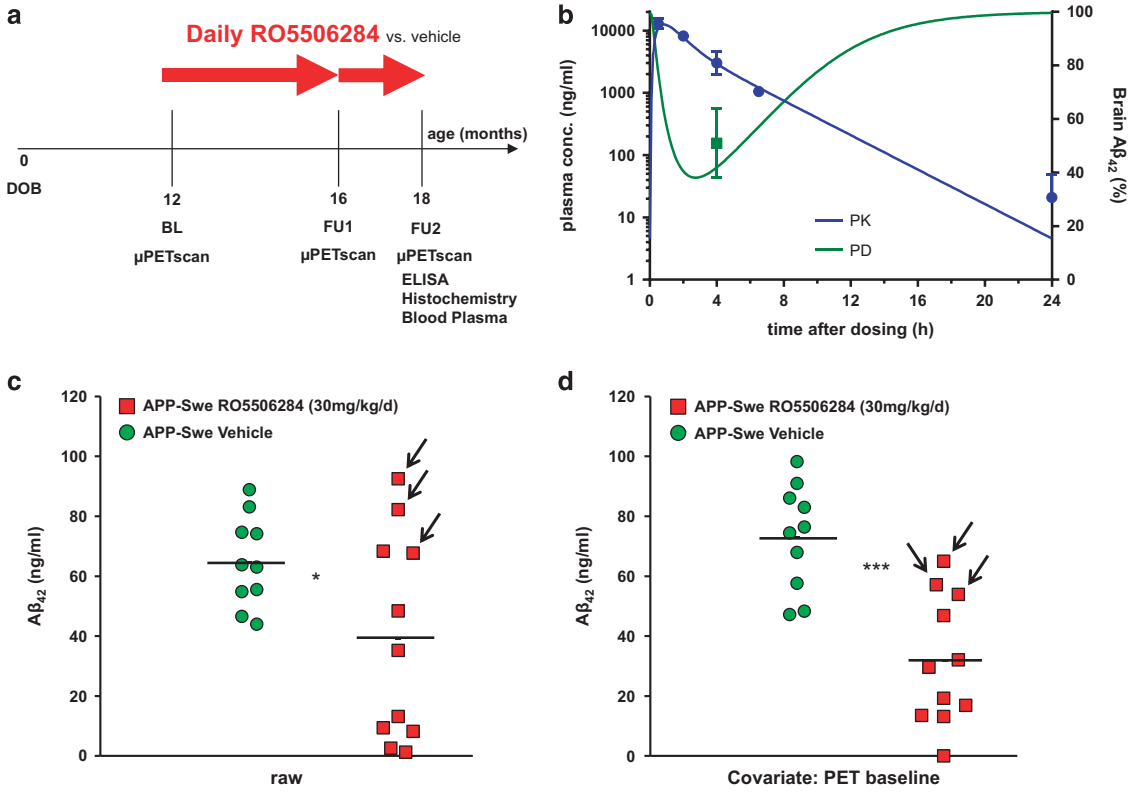

Figure 2. (**a**) Temporal overview of the chronic GSM treatment arm, lasting from 12 months to 18 months of age, with intermediate Aβ-PET at 16 months of age. (**b**) PK/PD simulation of brain $A\beta_{42}$ reduction effect after chronic treatment with 30 mg kg^{-1} daily of RO5506284. Blue curve indicates the PK simulation based on measured plasma concentrations (blue dots; mean value in ng $ml^{-1} \pm$ s.d., $n = 4$) after the last oral administration of the chronic treatment. Green curve shows simulated PD response in relation to a daily dose of 30 mg kg^{-1}. Area above the green curve represents the daily brain $A\beta_{42}$ reduction. Green square (mean value in percentage ± s.d., $n = 10$) shows the observed $A\beta_{42}$ levels after a single dose of 30 mg kg^{-1}. (**c**) Individual concentration of brain $A\beta_{42}$ after chronic treatment for 6 months without accounting for individual baseline amyloid levels. Each point represents the biochemically determined amount of $A\beta_{42}$ in one hemisphere of each transgenic mouse. Red indicates TG-GSM and green indicates TG-VEH mice. Arrows indicate the three animals of the TG-GSM group with elevated PET baseline estimates (>2s.d. above group mean). (**d**) Individual concentration of brain $A\beta_{42}$ after chronic treatment for 6 months upon adjustment by the individual baseline amyloid level, as assessed by Aβ-PET. Red indicates TG-GSM and green indicates TG-VEH mice. Arrows indicate the three animals of the TG-GSM group with elevated PET baseline estimates (>2s.d. above group mean). The horizontal line in the middle represents the mean value. *indicates statistically significant at $P < 0.05$; ***indicates statistically significant at $P < 0.001$.

other Aβ species again did not differ significantly. Overall, chronic RO5506284 treatment caused a robust reduction of brain Aβ deposition, with greatest influence on the $A\beta_{42}$ fraction.

Aβ-PET allows monitoring GSM efficacy *in vivo*

Besides demonstrating that RO5506284 is a potent GSM, substantially lowering brain $A\beta_{42}$ levels *in vivo* upon single or prolonged treatment, monitoring with non-invasive Aβ-PET imaging was performed (see Figure 2a), acquiring a total of 131 microPET recordings. This molecular imaging technique was applied with the intention to accommodate the large inter-individual differences in initial plaque load and kinetics, thus affording sensitive detection of individual treatment effects on amyloid plaque burden.

Baseline results showed a trend towards elevated $SUVR_{CTX/CBL}$ (+4.2%; $P = 0.11$) in the TG-GSM group compared with TG-VEH, mainly driven by the three individual animals mentioned above (labeled with arrows in Figure 3a). The rather high inter-animal variation of the amyloid plaque burden further supports the need of non-invasive techniques, which allows determining longitudinally the amyloid plaque load and kinetics in individual animals during a therapeutic study. Thus, as exemplified in Figure 3b: Animal #05 is one individual with high baseline amyloid level, which turned out to be less effectively treated, whereas animal #06 had low baseline Aβ, which did not accumulate further during follow-up, consistent with a good response to RO5506284 treatment. Animal #21 is a representative untreated individual, in which serial PET revealed a steady increase from a low baseline amyloid level. At study termination, mean $SUVR_{CTX/CBL}$ was 9.1% lower ($P < 0.05$) in the TG-GSM mice than in the TG-VEH group (Figure 3c). When considering the individual plaque load kinetics, Δ%-$SUVR_{CTX/CBL}$, remained nearly constant in the TG-GSM group during 6 months of RO5506284 treatment (+2.6 ± 6.1%), whereas Δ%-$SUVR_{CTX/CBL}$ in the TG-VEH group increased by +17 ± 7% ($P < 0.001$; Figure 3d). Neither group of WT mice showed any significant longitudinal changes in $SUVR_{CTX/CBL}$ (Table 1). Baseline $SUVR_{CTX/CBL}$ in the TG-GSM group correlated with Δ%-$SUVR_{CTX/CBL}$ ($r = 0.67$, $P < 0.05$), whereas Δ%-$SUVR_{CTX/CBL}$ results in the TG-VEH group showed no correlation with baseline $SUVR_{CTX/CBL}$ ($r = -0.03$, $P =$ non significant; Figure 3e). Therefore Aβ-PET allowed the prediction of individual treatment success upon chronic GSM administration.

Post mortem histochemical analyses confirm the Aβ-PET data

To confirm and extend the *in vivo* results, methoxy-X04 staining of fibrillar Aβ was performed after the final Aβ-PET scan to investigate whether chronic RO5506284 treatment has an impact on

Table 1. Comprehensive overview of the study groups, with baseline and follow-up parameters in all modalities

				Imaging			*Histology*			*Biochemistry*						
Study group	*Age months (scan)*	*Weight g ± s.d.*	n	$SUVR_{CTX/CBL}$ ± s.d.	Δ%-$SUVR_{CTX/CBL}$ ± s.d. vs BL	Δ%-$SUVR_{CTX/CBL}$ ± s.d. vs FU1	*Plaque load (percentage area ± s.e.m.)*	*Plaque load (percentage area ± s.e.m.) COVAR*	*Plaque density (N per mm³ ± s.e.m.)*	*Plaque density (N per mm³ ± s.e.m.) COVAR*	$Aβ_{38}$ *(ng ml⁻¹ ± s.e.m.)*	$Aβ_{38}$ *(ng ml⁻¹ ± s.e.m.) COVAR*	$Aβ_{40}$ *(ng ml⁻¹ ± s.e.m.)*	$Aβ_{40}$ *(ng ml⁻¹ ± s.e.m.) COVAR*	$Aβ_{42}$ *(ng ml⁻¹ ± s.e.m.)*	$Aβ_{42}$ *(ng ml⁻¹ ± s.e.m.) COVAR*	$Aβ_{tot}$ *(ng ml⁻¹ ± s.e.m.)*	$Aβ_{tot}$ *(ng ml⁻¹ ± s.e.m.) COVAR*
APP-Swe (RO5506284)	12 (BL)	27.2 ± 3.2	12	1.00 ± 0.05														
	16 (FU1)	26.8 ± 2.5	12	1.01 ± 0.06	+1.7 ± 3.9%													
	18 (FU2)	27.7 ± 2.6	11	1.03 ± 0.10[a]	+2.6 ± 6.1%[b]	+0.9 ± 6.5%[a]	3.4 ± 1.0	2.6 ± 0.5[a]	70.3 ± 21.2	55.8 ± 12.6[a]	13 ± 4	10 ± 2	146 ± 50	116 ± 33	39 ± 10[a]	32 ± 6[b]	198 ± 63	158 ± 40
APP-Swe (vehicle)	12 (BL)	26.4 ± 2.4	11	0.96 ± 0.04														
	16 (FU1)	26.5 ± 1.7	11	1.03 ± 0.05	+6.7 ± 6.8%													
	18 (FU2)	26.3 ± 1.5	9	1.13 ± 0.08	+17.1 ± 6.9%	+10.1 ± 9.7%	3.6 ± 0.6	4.5 ± 0.6	90.7 ± 11.3	107.9 ± 12.4	11 ± 2	15 ± 2	138 ± 24	174 ± 30	65 ± 5	73 ± 6	214 ± 28	261 ± 35
C57BL/6 (RO5506284)	12 (BL)	24.6 ± 1.1	11	1.02 ± 0.05														
	16 (FU1)	26.4 ± 1.2	10	1.00 ± 0.06	−2.1 ± 2.9%													
	18 (FU2)	26.7 ± 1.2	10	0.99 ± 0.06	−2.6 ± 3.3%	−0.3 ± 2.9%												
C57BL/6 (vehicle)	12 (BL)	24.2 ± 1.1	12	1.01 ± 0.06														
	16 (FU1)	24.8 ± 1.5	11	1.03 ± 0.04	+2.6 ± 3.9%													
	18 (FU2)	25.5 ± 1.1	11	1.02 ± 0.04	+2.0 ± 3.6%	−0.7 ± 2.7%												

Abbreviations: BL, baseline; COVAR, covariate; FU1, follow-up 1; FU2, follow-up 2; SUVR, standard-uptake-value ratios. Column 5 indicates the Aβ-PET $SUVR_{CTX/CBL}$ value for each scan time (baseline, follow-up 1, follow-up 2 (termination) scans), whereas column 6 indicates Δ%-$SUVR_{CTX/CBL}$ between follow-up and termination scans relative to the baseline value, and column 7 indicates Δ%-$SUVR_{CTX/CBL}$ between follow-up 1 and follow-up 2 results. Histochemically determined plaque load and plaque density of one brain hemisphere with and without including the PET baseline estimate as a covariate (COVAR) are presented in columns 8–11. Biochemical determination of insoluble $Aβ_{38}$, $Aβ_{40}$, $Aβ_{42}$ and $Aβ_{tot}$ concentrations in the other brain hemisphere with and without including the PET baseline estimate as a COVAR are presented in columns 12–19. [a]statistically significant at $P < 0.05$. [b]statistically significant at $P < 0.001$ for the contrast of TG-GSM and TG-VEH mice.

plaque load, density or size. Plaque load in the TG-GSM mice was reduced by 42% relative to the TG-VEH group ($P < 0.05$; Figure 4a), whereas plaque density was 48% lower in the TG-GSM group compared with TG-VEH mice ($P < 0.05$; Figure 4b). Furthermore, histogram plotting of plaque size revealed differing distributions between groups of TG mice, showing fewer ($P < 0.001$) small plaques (size $< 800\ \mu m^2$) in TG-GSM animals (Figure 4c). Reduced numbers of small plaques in TG-GSM animals is consistent with a primary effect of RO5506284 on *de novo* amyloidogenesis, as exemplified in mouse #5 and #6 with only few but rather large plaques, whereas the TG-VEH animal #21 had a considerable number of small plaques (Figure 4d).

Terminal measurements correlate highly across modalities

There was a high correlation between final Aβ-PET findings and plaque density ($r = 0.84$; $P < 0.001$; Figure 4e), plaque load ($r = 0.79$; $P < 0.001$; Supplementary Information), and insoluble $Aβ_{42}$ levels ($r = 0.83$; $P < 0.001$; Figure 4f) as assessed in the corresponding hemisphere. Likewise, insoluble $Aβ_{42}$ levels highly correlated with plaque density ($r = 0.81$; $P < 0.001$; Figure 4g) and plaque load ($r = 0.77$; $P < 0.001$; Supplementary Information) as assessed in the contralateral hemisphere.

DISCUSSION

This is the first large-scale longitudinal Aβ-PET study of cerebral amyloidosis in a transgenic AD mouse model treated with a chronic disease-modifying therapy. The study also entails corroborative histopathological, as well as biochemical analyses, thus encompassing three different readout modalities for monitoring amyloidogenesis. We found that daily oral GSM treatment commencing at 12 months attenuated the subsequent rate of *de novo* amyloidogenesis, which supports current thinking that early initiation of intervention should be most beneficial.

Aβ-PET improves detection of GSM effects by accounting for inter-animal variability and predicts outcome

We elected to start GSM treatment at the age of 12 months in consideration that discernible plaque formation is just barely evident in APP-Swe animals at the age of 9 months.[33] In general, individual plaque loads are quite heterogeneous in AD mouse models, most notably at an early age.[27,37] Starting treatment at 12 months, in order to accommodate the considerable variability of individual plaque loads, enabled us to predict response rates as a function of baseline plaque load with Aβ-PET. In the present APP-Swe mouse study, $Aβ_{42}$ levels, density of fibillar Aβ plaques and Aβ-PET signal at 18 months, all correlated well, and displayed comparable treatment effects in the contrast between TG-GSM and TG-VEH groups (Figure 4e–g). However, detection of the real longitudinal effect of GSM treatment was hampered by the slightly higher amyloidosis in the TG-GSM group at therapy initiation. We attribute this to chance, such that (after randomization) 3 of 12 mice of the TG-GSM cohort had an Aβ-PET signal at study baseline exceeding that in the saline-treated control group (>2 s.d.), indicating presence of established brain amyloidosis at only 12 months of age (Figure 3c). Despite RO5506284 treatment, the total Aβ levels at study termination were >30% higher in these three mice compared with any other TG mouse, indicating not only early onset, but also enhanced progression in these animals. High variability of the transgene expression is well known in this strain, and, indeed, among many transgenic AD mouse models.[33,37] This phenomenon indicates that larger group numbers may be necessary in order to obtain better group randomization; alternately, results of baseline Aβ-PET-scans could be used to allocate individuals to comparable groups prior to initiation of interventions. However, the present Aβ-PET design partially accommodates the imperfect randomization by

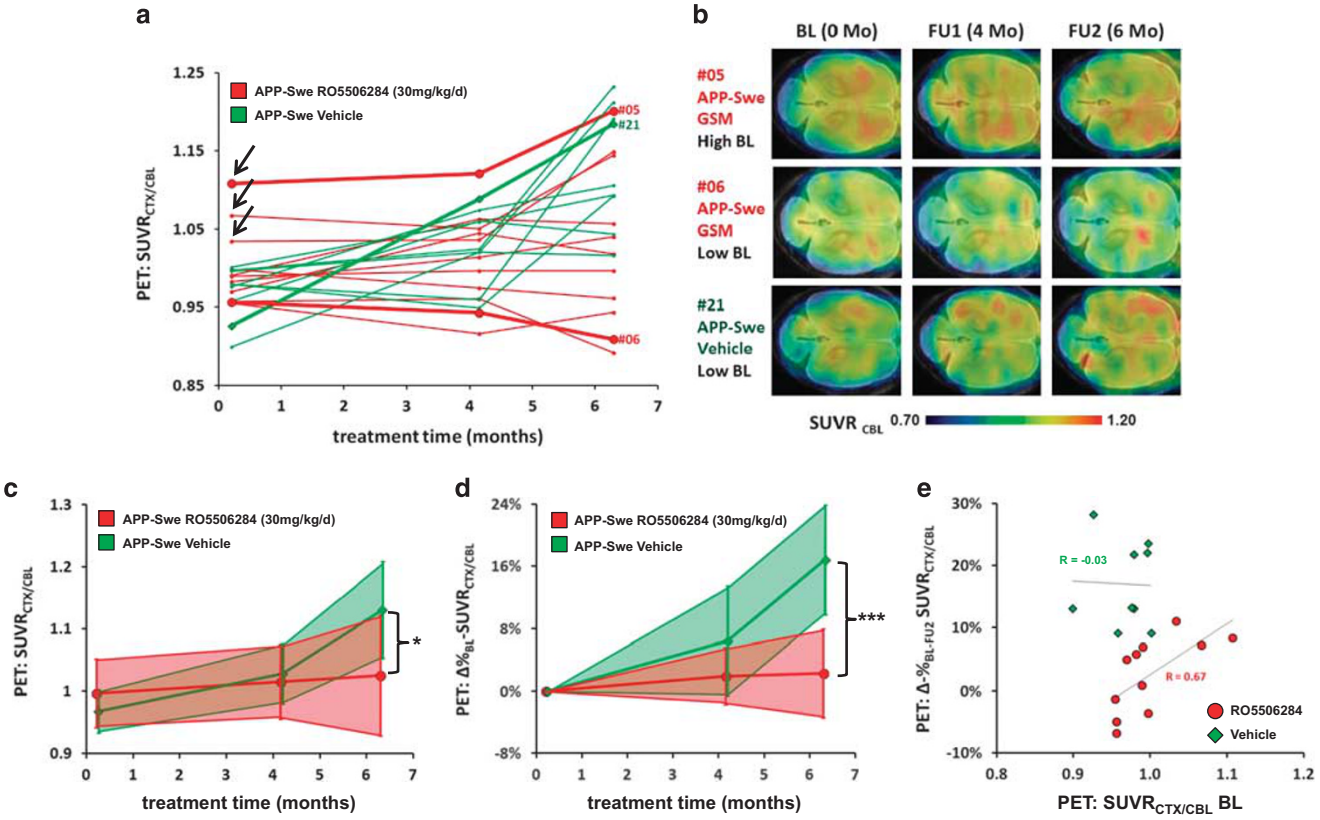

Figure 3. (**a**) Individual Aβ-PET estimates from baseline (12 months) to termination (18 months). Longitudinal courses of $SUVR_{CTX/CBL}$ for each mouse are depicted by individual lines. Symbols and lines for representative mice #5 and #6 (TG-GSM, red), as well as mouse #21 (TG-VEH, green) are accentuated. (**b**) Axial slices of Aβ-PET images from mice #5, #6 and #21 at each study point superimposed on an MRI atlas. (**c**) Absolute $SUVR_{CTX/CBL}$ values for each of the three PET scanning times are shown for TG-GSM (red) and TG-VEH (green) mice. The thick line marks the mean value, whereas the filled area indicates the s.d. for all mice. *indicates statistically significant at $P < 0.05$. (**d**) Percentage increase of follow-up and termination $SUVR_{CTX/CBL}$ relative to individual baseline values for TG-GSM (red) and TG-VEH (green) mice. The thick line marks the mean value, whereas the filled area indicates the s.d. of all mice. ***indicates statistically significant at $P < 0.001$. (**e**) Response prediction by means of Aβ-PET. The percentage increase from baseline to termination $SUVR_{CTX/CBL}$ is depicted as a function of the individual baseline value. For the TG-GSM, a low baseline value predicted a lesser increase in amyloidosis during treatment, whereas mice with a high baseline value had a high increase despite treatment. For the TG-VEH, there was a remarkable increase in $SUVR_{CTX/CBL}$, which was not a function of the individual baseline value. The correlations (*r*) between the percentage increase and the baseline value are indicated.

accounting for elevated baseline Aβ levels in three individuals through calculation of Δ%-$SUVR_{CTX/CBL}$, and by affording the possibility to adjust for the Aβ-PET baseline covariate in other histological and biochemical readouts. The longitudinal Aβ-PET approach sensitively detected the GSM treatment effects in the group as a whole, thus avoiding false–positive or false-negative results owing to the imperfect group randomization.

Our study revealed that high amyloid $SUVR_{CTX/CBL}$ at baseline Aβ-PET recordings correlated positively with further increases in Aβ-PET signal despite treatment. Those animals with a relatively low cortical Aβ-PET signal at treatment start still had relatively low plaque burden at study termination. These preclinical findings that pre-existing amyloidosis is a poor precondition for therapy response are consistent with failed treatment trials of symptomatic AD patients, in whom amyloidosis may already have run its course, or otherwise produced irreversible damage.[38–42]

Reduced $A\beta_{42}$ levels in RO5506284 treated APP-Swe mice primarily lead to inhibition of *de novo* amyloidogenesis

It is well known that of the various APP processing products $A\beta_{42}$ has a particularly high amyloidogenic potential and is responsible for the initiation of plaque formation.[43] Although our PK/PD analysis based on acute effect data suggested only 20–25% reduction of brain $A\beta_{42}$, over the treatment period we observed a significant effect on the amyloid pathology in the Tg2576 mouse model. Indeed, we found pronounced reductions (−56%; $P < 0.005$) of fibrillar Aβ plaques stained with methoxy-X04 in the TG-GSM group compared with TG-VEH at study termination. Significantly fewer small-sized plaques were seen in the TG-GSM animals, leading us to conclude that primarily *de novo* amyloidogenesis is sensitive to GSM treatment (Figure 4c). This positive result seems in line with a previous GSM treatment study in Tg2576 mice, which suggested that the modulator used in this study was likewise effective in inhibiting initiation of new Aβ plaques, but less effective in inhibiting the growth of pre-existing ones.[21] Our present findings of effects on amyloid protein levels are also consistent with other reports on preclinical GSM interventions. Thus, Rogers *et al.*[24] found a dose-dependent reduction of $A\beta_{42}$ and a decrease of total Aβ in Tg2576 mice treated with EVP-0015962 for 50 weeks. Imbimbo *et al.*[21] detected a reduction of $A\beta_{42}$ and a decrease of $A\beta_{40}$ in Tg2576 mice treated with CHF5074 for 17 weeks, whereas Kounnas *et al.*[22] found reduced $A\beta_{42}$, $A\beta_{40}$ and $A\beta_{38}$ in Tg2576 mice treated with a bridged-aromatic scaffold GSM for 7 months. Van Broeck *et al.*[25] administered antibodies against soluble and deposited Aβ, which

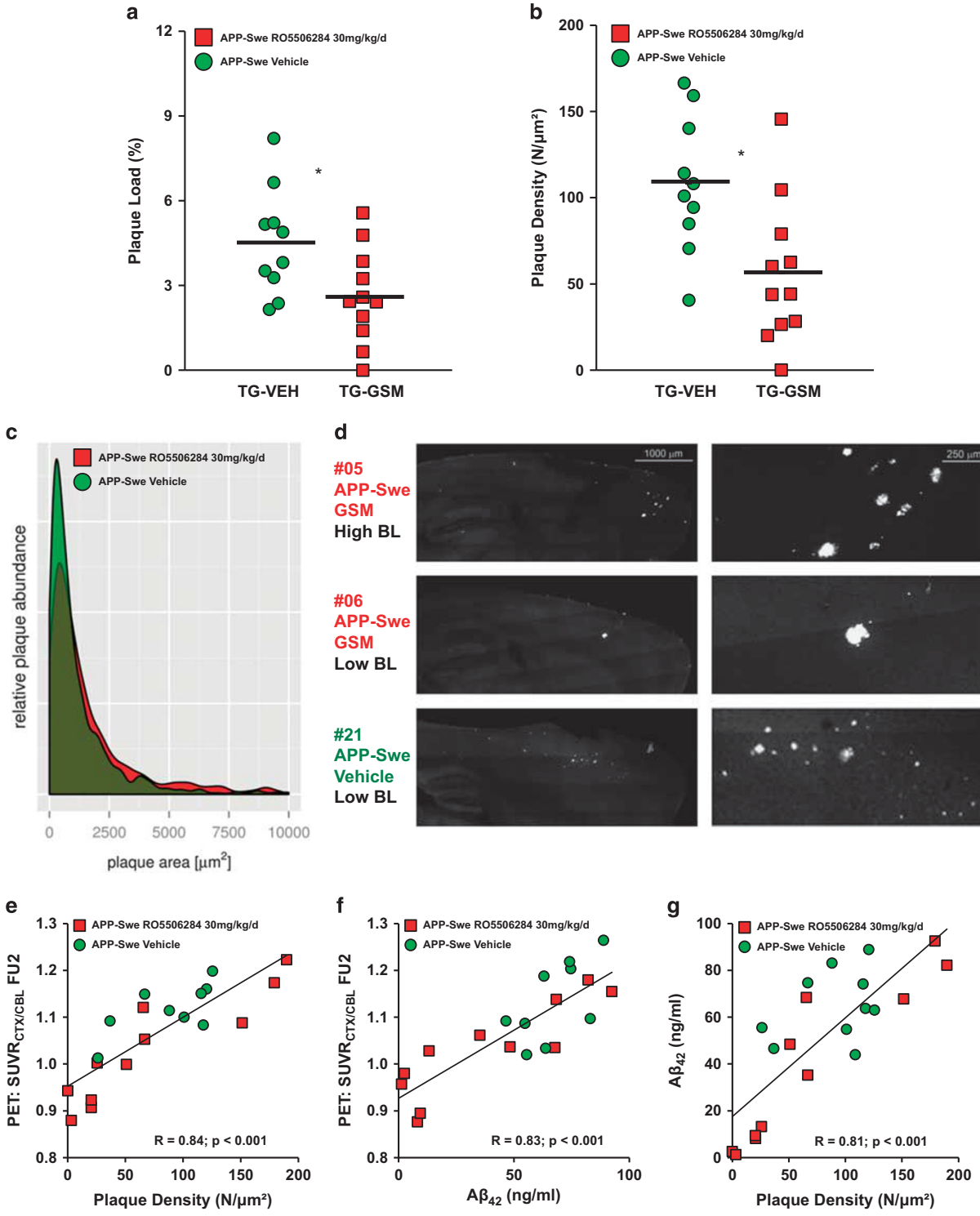

Figure 4. (**a**) Plaque load (%) in both TG groups assessed by methoxy-X04 staining. Each dot represents the histochemically determined plaque load, using Aβ-PET baseline estimate as covariate. Red indicates TG-GSM animals and green shows TG-VEH animals. (**b**) Plaque density using Aβ-PET baseline estimate as covariate for one hemisphere of each TG mouse. Red indicates TG-GSM animals and green shows TG-VEH animals. The horizontal line in the middle represents the mean value. *indicates statistically significant at $P < 0.05$. (**c**) Histogram plotting of plaque size revealed a differing distribution between groups of TG mice, with significantly fewer small plaques in the TG-GSM animals (red). (**d**) Methoxy-X04 staining of representative sagittal slices in the three above mentioned animals, the right panel zooms into the areas with the largest clusters of amyloid plaques in frontal parts of cerebral cortex. (**e**) Correlation of final Aβ-PET estimates and plaque density shows excellent agreement. Corresponding hemispheres were used from TG-GSM (red squares) and TG-VEH (green circles) animals for this comparison. (**f**) Correlation of final Aβ-PET estimates and insoluble $A\beta_{42}$ levels shows excellent agreement. Corresponding hemispheres were used from TG-GSM (red squares) and TG-VEH (green circles) animals for this comparison. (**g**) Correlation of $A\beta_{42}$ levels and plaque density shows excellent agreement. Contralateral hemispheres were used from TG-GSM (red squares) and TG-VEH (green circles) animals for this comparison.

evoked at 7 months, a dose-dependent decrease of $A\beta_{42}$, decreased $A\beta_{40}$ and a reduction of $A\beta_{38}$ in Tg2576 mice.

Recommendation for upcoming treatment trials targeting Aβ-pathology

Because a suitable antibody clears the existing Aβ deposits, whereas a GSM could also prevent *de novo* amyloidogenesis, we suppose that a combination treatment might prove even more efficacious than single treatment paradigms in reducing amyloidosis. Another important outcome of our study is that the serial assessment with Aβ-PET throughout the course of a long-term treatment study, in conjunction with histopathological and biochemical end point analyses, appears to be superior to simpler experimental paradigms, in which only the end point readouts are obtained. Given the well known inter-animal variability observed in this study, parallel Aβ-PET monitoring during the course of treatment, as well as normalization of results to baseline Aβ-PET makes the findings obtained at study end more robust and meaningful. We propose that application of serial Aβ-PET during treatment studies will allow for faster translation of disease-modifying approaches from the preclinical stage to the clinic.

Limitations

As we tested only a single dose up to 30 mg kg^{-1} of the GSM RO5506284, we cannot be certain that the maximum possible effect with minimum side effects was obtained. However, present results will provide the basis for designing a suitably powered dose-response study.

In addition, our design was not informative about protection against cognitive changes or impaired brain energy metabolism, as documented in a study by Martin-Moreno *et al*.[44] However, this does not detract for our major objective, which was to obtain serial Aβ-PET and terminal biochemical measurements of histological plaque load and Aβ levels in all animals.

CONCLUSION

This is the first large-scale serial Aβ-PET study during prolonged GSM treatment in a transgenic AD model. Multimodal data included biochemical and histopathological findings, in addition to the serial, non-invasive Aβ-PET investigations, which accommodated the large inter-individual differences in initial plaque load and kinetics, thus affording sensitive detection of treatment effects. Prediction of treatment response was facilitated by individual Aβ-PET measurements of baseline amyloid level. GSM treatment with RO5506284 attenuated *de novo* amyloidogenesis compared with vehicle, in line with the notion that early treatment initiation is most likely to be beneficial. The modalities applied should not be considered in competition but rather are complementary and add further value to any single modality alone.

CONFLICT OF INTEREST

CH is an advisor of F. Hoffmann-La Roche. JB, TL and KB are employees of F. Hoffmann-La Roche. PB and AR have received speaking honoraria from Piramal Imaging. The remaining authors declare no conflict of interest.

ACKNOWLEDGMENTS

This study was supported by the SyNergy Cluster (JH, PB, CH and AR) and by the European Research Council under the European Union's Seventh Framework Program (FP7/2007–2013)/ERC Grant Agreement No. 321366-Amyloid (advanced grant to CH). AJ was supported by the Foundation for Polish Science within the International PhD Project 'Studies of nucleic acids and proteins—from basic to applied research', co-financed by European Union—Regional Development Fund (MPD/2009-3/2). We thank Karin Bormann-Giglmaier and Rosel Oos for excellent technical assistance. Florbetaben precursor was kindly provided by Piramal Imaging. We thank Jaroslaw Dzbek for help in data processing.

REFERENCES

1 Ziegler-Graham K, Brookmeyer R, Johnson E, Arrighi HM. Worldwide variation in the doubling time of Alzheimer's disease incidence rates. *Alzheimers Dement* 2008; **4**: 316–323.
2 Braak H, Braak E. Neuropathological stageing of Alzheimer-related changes. *Acta Neuropathol* 1991; **82**: 239–259.
3 Haass C, Selkoe DJ. Soluble protein oligomers in neurodegeneration: lessons from the Alzheimer's amyloid beta-peptide. *Nat Rev Mol Cell Biol* 2007; **8**: 101–112.
4 Sun X, Jin L, Ling P. Review of drugs for Alzheimer's disease. *Drug Discov Ther* 2012; **6**: 285–290.
5 Reisberg B, Doody R, Stoffler A, Schmitt F, Ferris S, Mobius HJ. Memantine in moderate-to-severe Alzheimer's disease. *N Engl J Med* 2003; **348**: 1333–1341.
6 Herrmann N, Li A, Lanctot K. Memantine in dementia: a review of the current evidence. *Exp Opin Pharmacother* 2011; **12**: 787–800.
7 Dhillon S. Rivastigmine transdermal patch: a review of its use in the management of dementia of the Alzheimer's type. *Drugs* 2011; **71**: 1209–1231.
8 Wong GT, Manfra D, Poulet FM, Zhang Q, Josien H, Bara T *et al.* Chronic treatment with the gamma-secretase inhibitor LY-411,575 inhibits beta-amyloid peptide production and alters lymphopoiesis and intestinal cell differentiation. *J Biol Chem* 2004; **279**: 12876–12882.
9 Doody RS, Raman R, Farlow M, Iwatsubo T, Vellas B, Joffe S *et al.* A phase 3 trial of semagacestat for treatment of Alzheimer's disease. *N Engl J Med* 2013; **369**: 341–350.
10 De Strooper B. Lessons from a failed gamma-secretase Alzheimer trial. *Cell* 2014; **159**: 721–726.
11 Bittner T, Fuhrmann M, Burgold S, Jung CK, Volbracht C, Steiner H *et al.* Gamma-secretase inhibition reduces spine density *in vivo* via an amyloid precursor protein-dependent pathway. *J Neurosci* 2009; **29**: 10405–10409.
12 Blennow K, Zetterberg H, Haass C, Finucane T. Semagacestat's fall: where next for AD therapies? *Nat Med* 2013; **19**: 1214–1215.
13 Liebscher S, Page RM, Kafer K, Winkler E, Quinn K, Goldbach E *et al.* Chronic gamma-secretase inhibition reduces amyloid plaque-associated instability of pre- and postsynaptic structures. *Mol Psychiatry* 2014; **19**: 937–946.
14 Karran E, Mercken M, De Strooper B. The amyloid cascade hypothesis for Alzheimer's disease: an appraisal for the development of therapeutics. *Nat Rev Drug Discov* 2011; **10**: 698–712.
15 Weggen S, Eriksen JL, Das P, Sagi SA, Wang R, Pietrzik CU *et al.* A subset of NSAIDs lower amyloidogenic Abeta42 independently of cyclooxygenase activity. *Nature* 2001; **414**: 212–216.
16 Weggen S, Eriksen JL, Sagi SA, Pietrzik CU, Golde TE, Koo EH. Abeta42-lowering nonsteroidal anti-inflammatory drugs preserve intramembrane cleavage of the amyloid precursor protein (APP) and ErbB-4 receptor and signaling through the APP intracellular domain. *J Biol Chem* 2003; **278**: 30748–30754.
17 Ebke A, Luebbers T, Fukumori A, Shirotani K, Haass C, Baumann K *et al.* Novel gamma-secretase enzyme modulators directly target presenilin protein. *J Biol Chem* 2011; **286**: 37181–37186.
18 Jumpertz T, Rennhack A, Ness J, Baches S, Pietrzik CU, Bulic B *et al.* Presenilin is the molecular target of acidic gamma-secretase modulators in living cells. *PLoS One* 2012; **7**: e30484.
19 Ohki Y, Higo T, Uemura K, Shimada N, Osawa S, Berezovska O *et al.* Phenylpiperidine-type gamma-secretase modulators target the transmembrane domain 1 of presenilin 1. *EMBO J* 2011; **30**: 4815–4824.
20 Pozdnyakov N, Murrey HE, Crump CJ, Pettersson M, Ballard TE, Am Ende CW *et al.* gamma-Secretase modulator (GSM) photoaffinity probes reveal distinct allosteric binding sites on presenilin. *J Biol Chem* 2013; **288**: 9710–9720.
21 Imbimbo BP, Del Giudice E, Colavito D, D'Arrigo A, Dalle Carbonare M, Villetti G *et al.* 1-(3',4'-Dichloro-2-fluoro[1,1'-biphenyl]-4-yl)-cyclopropanecarboxylic acid (CHF5074), a novel gamma-secretase modulator, reduces brain beta-amyloid pathology in a transgenic mouse model of Alzheimer's disease without causing peripheral toxicity. *J Pharmacol Exp Ther* 2007; **323**: 822–830.
22 Kounnas MZ, Danks AM, Cheng S, Tyree C, Ackerman E, Zhang X *et al.* Modulation of gamma-secretase reduces beta-amyloid deposition in a transgenic mouse model of Alzheimer's disease. *Neuron* 2010; **67**: 769–780.
23 Sivilia S, Lorenzini L, Giuliani A, Gusciglio M, Fernandez M, Baldassarro VA *et al.* Multi-target action of the novel anti-Alzheimer compound CHF5074: in vivo study of long term treatment in Tg2576 mice. *BMC Neurosci* 2013; **14**: 44.
24 Rogers K, Felsenstein KM, Hrdlicka L, Tu Z, Albayya F, Lee W *et al.* Modulation of gamma-secretase by EVP-0015962 reduces amyloid deposition and behavioral deficits in Tg2576 mice. *Mol Neurodegener* 2012; **7**: 61.
25 Van Broeck B, Chen JM, Treton G, Desmidt M, Hopf C, Ramsden N *et al.* Chronic treatment with a novel gamma-secretase modulator, JNJ-40418677, inhibits amyloid plaque formation in a mouse model of Alzheimer's disease. *Br J Pharmacol* 2011; **163**: 375–389.

26 Manook A, Yousefi BH, Willuweit A, Platzer S, Reder S, Voss A *et al.* Small-animal PET imaging of amyloid-beta plaques with [11C]PiB and its multi-modal validation in an APP/PS1 mouse model of Alzheimer's disease. *PLoS One* 2012; **7**: e31310.
27 Rominger A, Brendel M, Burgold S, Keppler K, Baumann K, Xiong G *et al.* Longitudinal assessment of cerebral beta-amyloid deposition in mice overexpressing Swedish mutant beta-amyloid precursor protein using 18F-florbetaben PET. *J Nucl Med* 2013; **54**: 1127–1134.
28 Snellman A, Lopez-Picon FR, Rokka J, Salmona M, Forloni G, Scheinin M *et al.* Longitudinal amyloid imaging in mouse brain with 11C-PIB: comparison of APP23, Tg2576, and APPswe-PS1dE9 mouse models of Alzheimer disease. *J Nucl Med* 2013; **54**: 1434–1441.
29 Teipel SJ, Buchert R, Thome J, Hampel H, Pahnke J. Development of Alzheimer-disease neuroimaging-biomarkers using mouse models with amyloid-precursor protein-transgene expression. *Prog Neurobiol* 2011; **95**: 547–556.
30 Baumann K, Flohr A, Goetschi E, Green L, Jolidon S, Knust H *et al.* Preparation of heteroaryl substituted piperidines as β-amyloid modulators. US 20110201605 A1. 2011.
31 Kretner B, Fukumori A, Gutsmiedl A, Page RM, Luebbers T, Galley G *et al.* Attenuated Abeta42 responses to low potency gamma-secretase modulators can be overcome for many pathogenic presenilin mutants by second-generation compounds. *J Biol Chem* 2011; **286**: 15240–15251.
32 Brockhaus M, Grunberg J, Rohrig S, Loetscher H, Wittenburg N, Baumeister R *et al.* Caspase-mediated cleavage is not required for the activity of presenilins in amyloidogenesis and NOTCH signaling. *Neuroreport* 1998; **9**: 1481–1486.
33 Richards JG, Higgins GA, Ouagazzal AM, Ozmen L, Kew JN, Bohrmann B *et al.* PS2APP transgenic mice, coexpressing hPS2mut and hAPPswe, show age-related cognitive deficits associated with discrete brain amyloid deposition and inflammation. *J Neurosci* 2003; **23**: 8989–9003.
34 Page RM, Baumann K, Tomioka M, Perez-Revuelta BI, Fukumori A, Jacobsen H *et al.* Generation of Abeta38 and Abeta42 is independently and differentially affected by familial Alzheimer disease-associated presenilin mutations and gamma-secretase modulation. *J Biol Chem* 2008; **283**: 677–683.
35 Klunk WE, Bacskai BJ, Mathis CA, Kajdasz ST, McLellan ME, Frosch MP *et al.* Imaging Abeta plaques in living transgenic mice with multiphoton microscopy and methoxy-X04, a systemically administered Congo red derivative. *J Neuropathol Exp Neurol* 2002; **61**: 797–805.
36 Hahn S, Bruning T, Ness J, Czirr E, Baches S, Gijsen H *et al.* Presenilin-1 but not amyloid precursor protein mutations present in mouse models of Alzheimer's disease attenuate the response of cultured cells to gamma-secretase modulators regardless of their potency and structure. *J Neurochem* 2011; **116**: 385–395.
37 Teipel SJ, Buchert R, Thome J, Hampel H, Pahnke J. Development of Alzheimer-disease neuroimaging-biomarkers using mouse models with amyloid-precursor protein-transgene expression. *Prog Neurobiol* 2011; **95**: 547–556.
38 Coric V, van Dyck CH, Salloway S, Andreasen N, Brody M, Richter RW *et al.* Safety and tolerability of the gamma-secretase inhibitor avagacestat in a phase 2 study of mild to moderate Alzheimer disease. *Arch Neurol* 2012; **69**: 1430–1440.
39 Fleisher AS, Raman R, Siemers ER, Becerra L, Clark CM, Dean RA *et al.* Phase 2 safety trial targeting amyloid beta production with a gamma-secretase inhibitor in Alzheimer disease. *Arch Neurol* 2008; **65**: 1031–1038.
40 Golde TE, Koo EH, Felsenstein KM, Osborne BA, Miele L. gamma-Secretase inhibitors and modulators. *Biochim Biophys Acta* 2013; **1828**: 2898–2907.
41 Green RC, Schneider LS, Amato DA, Beelen AP, Wilcock G, Swabb EA *et al.* Effect of tarenflurbil on cognitive decline and activities of daily living in patients with mild Alzheimer disease: a randomized controlled trial. *JAMA* 2009; **302**: 2557–2564.
42 Yu Y, Logovinsky V, Schuck E, Kaplow J, Chang MK, Miyagawa T *et al.* Safety, tolerability, pharmacokinetics, and pharmacodynamics of the novel gamma-secretase modulator, E2212, in healthy human subjects. *J Clin Pharmacol* 2014; **54**: 528–536.
43 Younkin SG. The role of A beta 42 in Alzheimer's disease. *J Physiol Paris* 1998; **92**: 289–292.
44 Martin-Moreno AM, Brera B, Spuch C, Carro E, Garcia-Garcia L, Delgado M *et al.* Prolonged oral cannabinoid administration prevents neuroinflammation, lowers beta-amyloid levels and improves cognitive performance in Tg APP 2576 mice. *J Neuroinflammation* 2012; **9**: 8.

Supplementary Information accompanies the paper on the Molecular Psychiatry website (http://www.nature.com/mp)